Available online at www.sciencedirect.com
ScienceDirect
Acta Materialia 59 (2011) 2749–2761
Acta MATERIALIA
www.elsevier.com/locate/actamat

Use of nanoindentation to measure residual stresses in surface layers

J. Dean [a], G. Aldrich-Smith [b], T.W. Clyne [a,*]

[a] Department of Materials Science & Metallurgy, Cambridge University, Pembroke Street, Cambridge CB2 3QZ, UK
[b] AWE, Aldermaston, Reading, Berks RG7 4PR, UK

Received 28 May 2010; received in revised form 4 January 2011; accepted 5 January 2011

Abstract

Equal biaxial residual stresses (of up to about 175 MPa) have been generated in thin copper foils via differential thermal contraction. These foils were subsequently indented, under displacement control, and the load–displacement–time characteristics were measured. The applied load required for penetration to a given depth (in a given time) was found to decrease with increasing (tensile) residual stress, in accordance with predictions from a finite-element model (incorporating both plasticity and creep). The main thrust of this paper concerns sensitivities. Relatively small changes in residual stress (of the order of a few tens of MPa) were observed to generate effects that should be detectable via their influence on the nanoindentation response. This is encouraging in terms of the potential of the technique for characterizing (in-plane) residual stresses in surface layers, particularly for mapping of point-to-point variations (as opposed to obtaining accurate absolute values). In contrast to this, it is shown that changes in the hardness, as a consequence of changes in residual stress level, are smaller and more difficult to analyse.

Keywords: Nanoindentation; Finite-element analysis; Residual stresses; Non-destructive testing

1. Introduction

The indentation response of the near-surface region of a specimen should be affected by the presence of (in-plane) residual stresses, which will in general influence the yielding and plastic straining characteristics. It has previously been proposed that these stresses could be detected and measured using nanoindentation. This is an attractive concept, since it would allow such residual stresses to be measured quickly, and in a non-destructive manner, and possibly for them to be mapped over the surface of a component—for example, across a weld.

Tsui et al. [1] investigated the influence of (residual) stresses, created via an imposed bending moment, on the hardness (H) and Young's modulus (E) values obtained using nanoindentation. No dependence of E on residual stress levels is expected, and indeed the experimental data indicated this (after a correction had been made for the measured contact area). However, the hardness, which in general should be affected by residual stresses (assuming that they have a deviatoric component), was also found to be unaffected by them, after such a correction had been made. However, their data were quite noisy and in general the sensitivity to the levels of residual stress induced was rather poor in these experiments. Other workers [2–4] have detected changes in hardness with applied residual stress.

Tsui et al. [1] suggested that, when pile-up occurs, conventional methods for measuring hardness are prone to error, and indeed this is clearly possible, since uncertainties can arise concerning the true area of contact between indenter and specimen. In fact, any analysis that relies solely on the indenter area function is likely to suffer from this limitation—at least for indentation into materials that exhibit significant pile-up. However, in an accompanying paper [5], the same authors presented finite-element modelling (FEM) simulations suggesting that hardness is

* Corresponding author. Tel.: +44 1223 334332; fax: +44 1223 334567.
E-mail address: twc10@cam.ac.uk (T.W. Clyne).

1359-6454/$36.00 © 2011 Acta Materialia Inc. Published by Elsevier Ltd. All rights reserved.
doi:10.1016/j.actamat.2011.01.014

expected to be independent of residual stress, except in the case of large (tensile) residual stresses.

Xu and Li [6] reported, in a purely theoretical (FEM) study, that a slight decrease in H (obtained by nanoindentation) is expected with increasing (tensile) residual stress. They suggested that the ratio h_f/h_{max}, where h_f is the residual indent depth and h_{max} is the maximum indenter depth, could be an alternative measurement that might be more sensitive to the presence of residual stresses. They also showed that this ratio is larger for compressive (in-plane) residual stresses than for tensile stresses. The differences were more pronounced for materials with low values of E/σ_Y.

Suresh and Giannakopoulos [7] suggested comparing differences in the contact area between stressed and unstressed material, when indented to the same depth. No experimental data were provided. This approach has largely been dismissed as a viable method [4,8], at least for sharp indenters, since the theoretically predicted differences were relatively small (except for residual stresses approaching the yield stress).

Taljat and Pharr [3] suggested that the effects of residual stress would be more readily detectable if blunt, spherical indenters were employed, since the transition between elastic and plastic regimes is then more progressive. In a purely theoretical (FEM) study, they found that the mean contact pressure was more sensitive to residual stress (magnitude and sign) during the elastic–plastic transition, i.e. at intermediate indentation depths. At low depths (i.e. low contact area A), for which the deformation was purely elastic, the mean pressure was insensitive to residual stresses. For large A, the mean contact pressure was also insensitive to residual stress, because plasticity was fully developed and the deformation was dominated by large plastic strains. This may suggest that, as indentation deformation proceeds, the local plastic flow, which dominates the response of the material, so greatly affects the stress state around the indenter that the residual stress exerts a diminishing contribution with indenter depth. Of course, prediction of the details of the evolving stress field (and its interaction with an applied residual stress) does require numerical modelling.

Swadener et al. [4] developed two methods for determining biaxial residual stresses from indentation data. In the first method, the onset of yielding with applied residual stress was investigated. They noted, however, that yielding initiated at low indentation depths, where displacement measurements were imprecise. The onset of yielding was instead determined using least-square regression curve fits to experimental h_f/h_{max} data—yielding initiates at $h_f/h_{max} = 0$. Applied tensile stresses encouraged the early onset of yielding. Applied compressive stresses inhibited yielding. For their second method, Swadener et al. [4] had earlier noted that the mean contact pressure for various values of the contact area were offset from one another by an amount very close to the applied residual stress (at least in the elastic–plastic transition regime). Using an empirically derived expression relating biaxial stresses to the mean contact pressure and a constraint factor (modified to account for the applied residual stress), the biaxial residual stresses could be calculated. However, this method is unlikely to be universally applicable.

The methods developed by Swadener et al. [4] were applied by Lepienski et al. [8] to the study of residual stresses in thin films (5–7 μm). They found that these methods were not readily applicable to thin films, for three reasons: (i) obtaining a structurally equivalent reference specimen, with a known stress state, was difficult; (ii) surface roughness values were similar to indentation depths; and (iii) the presence of the substrate influenced the deformation of the film. Reducing the size of the indenter to eliminate substrate effects exacerbates the surface roughness issue.

The shape of the measured load–displacement curve has also been investigated. Lee and Kwon [9] found, for indentation into elastically strained single-crystal tungsten ((100) surfaces), that, for the same applied peak load, the indentation curves shift to lower (compressive) and higher (tensile) depths with applied residual stress. For a fixed prescribed indentation depth [1] the load–displacement curves were found to shift upwards (compressive), and downwards (tensile), with applied residual stress. These observations are in accordance with expectations.

Of course, both sensitivity and noise are of critical importance in this context. What is required is a technique in which the measurements being made are sensitive to relatively small changes in residual stress, with the associated noise being sufficiently low to ensure that the data are reliable. In general, no procedure has previously been identified which can be employed with any confidence to measure (local) residual stress levels using nanoindentation. The present paper is aimed at identifying how best to make and interpret such measurements, with both experimental and predicted (FEM) data being presented, and at obtaining insights into the sensitivities involved. The measurements have been made on copper foils bonded to massive copper or titanium substrates, with temperature changes being used to induce well-defined (equal biaxial) residual stresses in the foils, as a consequence of differential thermal contraction.

2. Experimental procedures

2.1. Material and specimen production

The experimental work in this study has been conducted on oxygen-free high-conductivity copper foil. A photomicrograph of the microstructure is shown in Fig. 1. The small grain size (relative to the indentation size) is advantageous, since multiple grains are indented and anisotropic deformation, associated with orientation-dependent slip, is avoided. (Of course, the material may still be anisotropic, but the indentation response should be representative of that of the foil as a whole.) Foils (50 μm in thickness) were attached to either Cu or Ti substrates (10 × 10 × 5 mm),

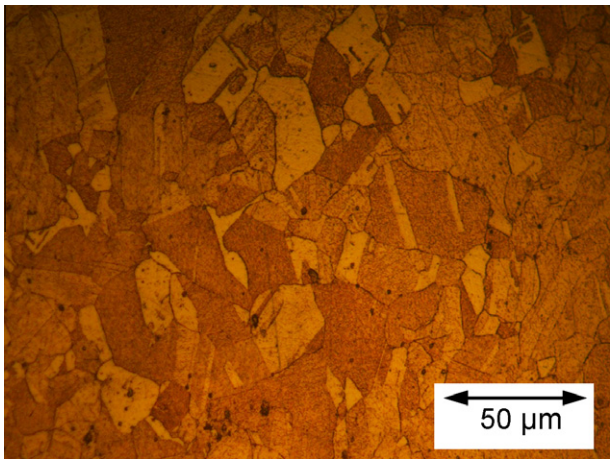

Fig. 1. Optical micrograph of the microstructure of the Cu foil (in-plane surface), after etching with dilute ferric chloride.

using a high-temperature araldite adhesive (Araldite® 2014 Structural Adhesive, Huntsman). The substrate materials were cut using electric discharge machining (EDM). In order to facilitate good adhesion between the substrates and the Cu foil, two steps were taken during specimen preparation: (i) the surfaces of the substrates were grit-blasted with alumina particles (~360 μm diameter), using a modified Guyson Euro 2SF sand-blaster, with an inlet pressure of 100 psi; and (ii) the contact face of the Cu foils were lightly abraded, using silicon carbide paper and light manual pressure. Both substrate and foil materials were cleaned afterwards with acetone.

The araldite was applied to the (grit-blasted) surface of the substrate. In order to minimize the thickness of the adhesive layer, the araldite was first heated over a hot-plate. The consequent reduction in the viscosity of the araldite was sufficient to allow a thin, continuous layer to form. After addition of the Cu foil, the araldite was allowed to cure for 24 h at room temperature.

The free surfaces of the Cu foils were polished, using conventional mechanical polishing procedures, with a final polish using 0.06 μm colloidal silica. Care was taken to ensure that the foil thickness was not substantially reduced during polishing. A profilometer scan, obtained using a "Talysurf" profilometer, is shown in Fig. 2; this profile confirms that the residual foil thickness is ~40 μm. The profilometer data also confirm that the adhesive layers were thin (~10–15 μm). The "lip" in the profile at the edge of the Cu foil was created during the cutting operation required to produce the "multi-level" specimen, but this feature would obviously not be present in normal specimens.

2.2. Stress–strain relationship for copper foil

Foils were machined, using EDM, to a geometry suitable for tensile testing (with a waisted central section), and tested in a customized low-load testing set-up, with displacements being measured using a scanning laser extensometer. Testing was carried out in both rolling and transverse directions. Typical data are shown in Fig. 3, where it can be seen that the foil exhibits little in-plane anisotropy. It is clear from the mechanical test results that the Cu foil is relatively brittle; for a heavily cold-rolled foil, such as the one employed, this is not surprising. However, it is the mechanical properties of the foil in the through-thickness direction (i.e. along the indentation axis) that are of prime interest here.

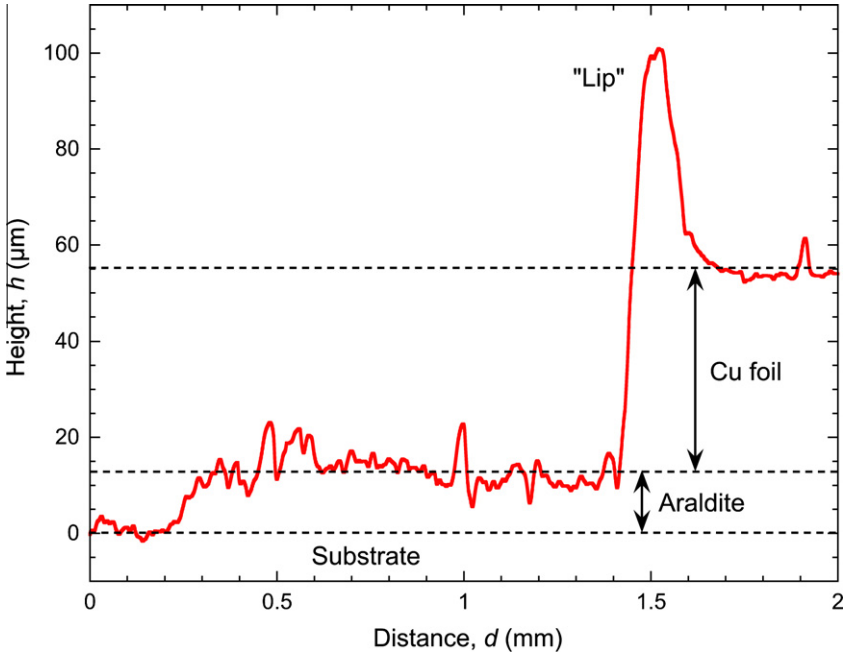

Fig. 2. Profilometer data from a scan across a specimen surface, showing that the thickness of the araldite layer is ~10–15 μm, while that of the Cu foil is ~40 μm.

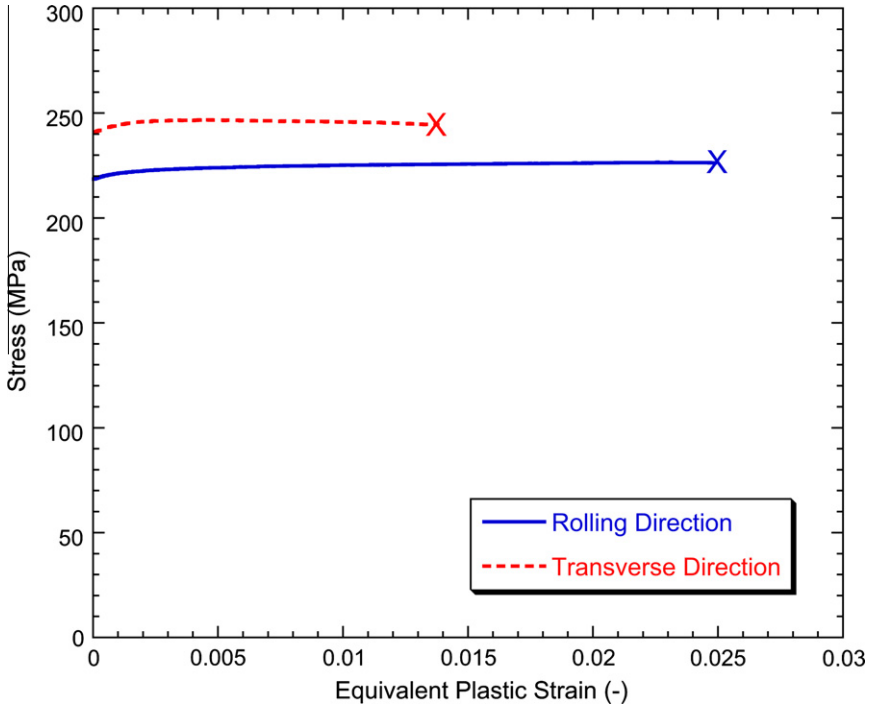

Fig. 3. Experimental stress–strain data for tensile testing of the Cu foil, in the rolling and transverse directions

2.2.1. Through-thickness yield stress

In order to determine the through-thickness yield stress, circular specimens were punched from the foil (11 mm diameter). These discs were then compressed between flat platens of silicon carbide, using an Instron servohydraulic mechanical testing machine. The specimens were lubricated with molybdenum disulfide, in order to minimize any constraints on deformation. Prior to compression, the specimen thickness was measured using a micrometer. Several samples were compressed, each to an increasing maximum load (with 10 MPa increments), at a displacement rate of 1 μm min^{-1}. After each test, the specimen thickness was measured once more. At 310 MPa, the foil thickness remained unchanged, i.e. the deformation was purely elastic. At 320 MPa, the foil thickness had decreased. A further series of experiments were conducted at 1 MPa increments, and the yield stress was estimated to be 315 MPa. It was not really possible, using this method, to investigate the through-thickness strain-hardening behaviour. Furthermore, it must be recognized that the precision to which the yield stress can be established in this way is in practice rather limited (perhaps ~±5–10%).

2.3. Creep behaviour

Specimens for creep testing were machined by EDM, and loaded in uniaxial tension (in the plane of the foil). Testing was carried out at room temperature and at 50 °C, for a range of stresses ($\sigma = 57.8$, 87.8, 137.8 and 187.8 MPa), under load control (a weight acting under gravity). The displacements were measured using a scanning laser extensometer, with a resolution of about 2–3 μm.

2.4. Residual stress generation

Residual stresses were generated in the foil by differential thermal contraction. The specimens were first heated in a (Lenton Thermal Designs ECF 12/3) furnace. This heating creates (equal biaxial) stress in the Cu foil on the Ti substrate, as a result of the differential thermal expansion misfit strain, which can be assumed to be accommodated entirely within the foil, since the substrate is massive. (There would also be a misfit strain, and consequent stresses, in the araldite layer: however, since this is also thin compared with the substrate, it would have no effect on the foil–substrate misfit strain.) Obviously, no such stresses are created in the foils on Cu substrates. Specimens were then held at the temperature concerned for a period of 1 h, with a surface coating of a grease used for the higher temperatures, to minimize oxide film formation. This period was sufficient (see Section 3.3.1) to allow these stresses in the foils to fully relax, due to creep deformation.

The specimens were then quenched, by immersing them in water at ambient temperature. During quenching, residual stresses were (once more) generated in the foils (on Ti substrates), as a result of the differential thermal contraction misfit strain. These stresses were tensile (since the thermal expansivity of Cu is greater than that of Ti). After quenching, the specimens were dried and transferred to the indenter specimen stage, where they were tested (with several indents being made on each specimen). There was thus a period of about 10 min between quenching and the start of testing, which itself took about 5–10 min. During this period, the residual stresses may relax (creep). This relaxation was simulated via FEM. It was found that it

did have a significant effect on the stress levels, even at this relatively low temperature and in the short period before testing (see Section 3.3.1). However, the relaxation was much less complete than in the period of an hour at the higher temperatures, and substantial stress levels were retained during the indentation.

Provided the elastic constants are known (and the system remains elastic), the (equal biaxial) stress level created by a temperature change in a system with this geometry is given by:

$$\sigma_r = \frac{\Delta\alpha\Delta T E_f}{(1-\nu_f)} \quad (1)$$

where E_f and ν_f are respectively the Young's modulus and Poisson ratio of the Cu foil, $\Delta\alpha$ is the difference in thermal expansivity between foil and substrate, and ΔT is the temperature change. Several values for ΔT have been employed, for both Cu and Ti substrates. The corresponding residual stresses, obtained using Eq. (1), are shown in Table 1. The elastic constants and thermal expansivities of the materials used are shown in Table 2. Also shown in Table 1 are the residual stresses after 10 min of relaxation at room temperature, as obtained by FEM modelling (see Section 3.3.1).

2.5. Indentation procedure

Nanoindentation testing was carried out using a MicroMaterials Ltd. Nanotest, which is a pendulum-based depth-sensing nanoindenter. A loading rate of 10 mN s^{-1} was employed. It has been shown elsewhere [10] that this loading rate is sufficiently fast to ensure that (pure) Cu will not experience significant amounts of creep deformation during such loading. Indentation was arrested at a depth of 1.65 μm. The load at this point was then maintained for a period of 50 s. This is designed to create some relaxation of the stresses by creep and hence ensure that the unloading response is purely elastic (not influenced by inelastic phenomena such as creep). The unloading rate was also 10 mN s^{-1}. Load–displacement–time data were acquired during indentation. Nine indentations were performed on each specimen. It was confirmed by visual inspection that, in each case, the indent straddled several grains. (It has been shown [10] that, if this is not the case, then the scatter in measured load is considerably greater and the average value does not reflect the macroscopic yielding and work-hardening behaviour of the material.)

2.6. Characterization of the indenter tip

The shape of the indenter tip was characterized using a Veeco Dimension 3100 atomic force microscopy (AFM) system, with an XY closed-loop scanner using Tapping-Mode™ with RTESPs (rotated tapping etched silicon probes). After locating the surface and apex of the indenter tip, 512 × 512 pixel scans of 15 μm × 15 μm were performed. Projected area functions were extracted from the data, using height histograms.

3. FE model formulation

Two FE models have been created. The first was developed in order to explore creep deformation during the 1 h holding period at elevated temperature and also the period of 10 min after quenching to room temperature that preceded indentation testing, as described in Section 2.4. The second was developed to simulate the indentation process.

3.1. Creep relaxation model

3.1.1. Meshing of the specimen and mechanical boundary conditions

A three-dimensional model was generated in ABAQUS to model creep relaxation during the holding period at elevated temperature, and also at room temperature (25 °C) after quenching (Section 2.4). Substrate, araldite and foil materials were modelled as deformable bodies, and meshed with eight-noded thermally coupled (temperature–displacement) brick elements (C3D8T). The substrate, araldite and foil were rigidly bonded at the interfaces.

3.1.2. Constitutive relations and creep parameters

Experimental creep strain data are shown in Fig. 4, for 25 and 50 °C, together with corresponding fitted curves. These were all obtained using an expression of the form:

$$\varepsilon_{creep} = A + B\log(t) \quad (2)$$

in which the values of A and B are given by:

$$A = C + D\sigma + E\sigma^2 \quad (3)$$

Table 1
Values of ΔT employed experimentally and corresponding in-plane residual stress levels created by differential thermal contraction of a Cu foil on a Ti substrate, obtained either using Eq. (1) or via FEM of the effect of creep relaxation (remote from specimen edges) after 10 min at room temperature.

ΔT (K)	Residual stress (MPa)	
	Eq. (1)	FE model
25	31.3	18
50	62.7	47
75	94.0	72
100	125.4	96
200	250.8	174

Table 2
Elastic constants and thermal expansivities of the materials used.

Material	Young's modulus, E (GPa)	Poisson ratio, ν (−)	Thermal expansivity, α (K^{-1})
Cu	110	0.342	16.4×10^{-6}
Ti	116	0.3	8.9×10^{-6}
Epoxy	4	0.38	45×10^{-6}

$$B = F + G\sigma + H\sigma^2 \quad (4)$$

The values used for the constants in these two expressions are given in Table 3. It can be seen that these fitted curves represent the experimental data quite well, and can be used for any stress level (within the range of the experiments).

Of course, these data relate to the behaviour from the beginning of creep, i.e. they represent primary creep. It can be seen in Fig. 4 that a steady creep rate (stage II) becomes established only after about 30 min or so. Clearly, it would be highly inaccurate if any attempt were made to simulate this relaxation behaviour on the basis of steady-state creep rates. The creep behaviour represented by Eq. (2) was implemented in ABAQUS using the user-subroutine CREEP, which is a general framework for defining time-dependent viscoplastic behaviour.

A power law (steady-state) creep model was, however, employed to model creep relaxation in the araldite layer. The creep strain rate is given by [11]:

$$\frac{d\varepsilon_{creep}}{dt} = A\sigma^n t^m \quad (5)$$

where t is the total time and A, n and m are user-defined material parameters. Values of these constants, for a similar two-component, cold-cure epoxy, were obtained from Yu et al. [12] and are listed in Table 4. (In fact, while creep will tend to occur in the adhesive, it will not influence the stress in the Cu foil, which will remain constrained to retain the in-plane dimensions of the substrate: nevertheless, this creep was included in the model for completeness.)

3.2. Indentation model

3.2.1. Meshing of the specimen and mechanical boundary conditions

An axisymmetric model was employed in ABAQUS to model the indentation experiments. This is acceptable here, since the residual stresses, the material properties (see Fig. 3) and the imposed loading are all isotropic in the plane of the specimen surface. The implicit solver was used for all simulations. The foil (40 μm thick), araldite (15 μm thick) and substrate (40 μm) layers were modelled as deformable bodies and meshed with 6311 linear quadrilateral elements (type CAX4R). The mesh was refined directly beneath the indenter. A sensitivity analysis was carried out, in order to confirm that this mesh was sufficiently fine to achieve convergence, numerical stability and mesh-independent results. The mesh is shown in Fig. 5.

The indenter was modelled as an analytical rigid body, with dimensions consistent with the AFM-determined area function (Section 2.6). In fact, the AFM measurements indicated that the indenter tip had a shape very close to that of a sphere, but with a radius of 13 μm, rather than the nominal value of 10 μm. Both spheres are shown in Fig. 5. For all simulations, a rigid 13 μm radius sphere was employed. A maximum displacement of 1.65 μm was specified as a boundary condition, corresponding to the maximum penetration depth in the experiments. Interfacial friction between the indenter and the surface of the Cu foil was neglected [10].

Table 3
Fitting parameters for representation of the (primary) creep strain behaviour (Fig. 4).

Parameter	Temperature	
	25 °C	50 °C
C (−)	-1.75×10^{-4}	-1.41×10^{-3}
D (MPa^{-1})	1.70×10^{-6}	2.21×10^{-5}
E (MPa^{-2})	-2.07×10^{-8}	-1.48×10^{-7}
F (−)	4.54×10^{-5}	4.52×10^{-4}
G (MPa^{-1})	7.06×10^{-7}	-2.25×10^{-6}
H (MPa^{-2})	6.01×10^{-9}	5.10×10^{-8}

3.2.2. Incorporation of residual stresses

Prior to the indentation step, a mechanical displacement of the foil was prescribed at the lateral boundary of the model. These displacements were designed to generate residual stresses of the same magnitudes as those created by the heating and quenching operations (see Table 1).

3.2.3. Elastic constants and constitutive relation

The elastic constants for the Cu foil, the epoxy resin and the Ti substrate are given in Table 2. The constitutive relation employed for the Cu foil was:

$$\sigma = \sigma_Y + k\varepsilon \quad (6)$$

in which σ_Y is the yield stress and k is the work-hardening rate. The values of these parameters for the Cu foil in the through-thickness direction are not accurately known, although the experimentally estimated value for σ_Y of 315 MPa (see Section 2.2) is certainly a good starting point. It also seems likely that a value for k of 0 should be at least a fair approximation, in view of the observed in-plane behaviour (Fig. 3), with the stress remaining more or less constant up until fracture. Of course, tensile testing was only carried out up to the failure strain of ~2.5%, whereas, within the indentation model, the stress states experienced by individual volume elements are largely compressive, and plastic strains extend up to about 100%. However, it is expected that the relationship will be similar in tension and compression, and that it will apply up to large (compressive) strains. In addition to the "reference" case of $\sigma_Y = 315$ MPa and $k = 0$ MPa, simulations were also carried out to explore the effects of changing these two values.

3.2.4. Prediction of hardness

The hardness is obtained as the ratio of the applied load to the projected area of contact at peak indentation depth. Experimentally, this area is conventionally found from the

Table 4
Steady-state creep parameter values for an epoxy resin [12].

A (MPa^{-n} s$^{-(1+m)}$)	n (−)	m (−)
1.02×10^{-10}	0.5756	4.0438

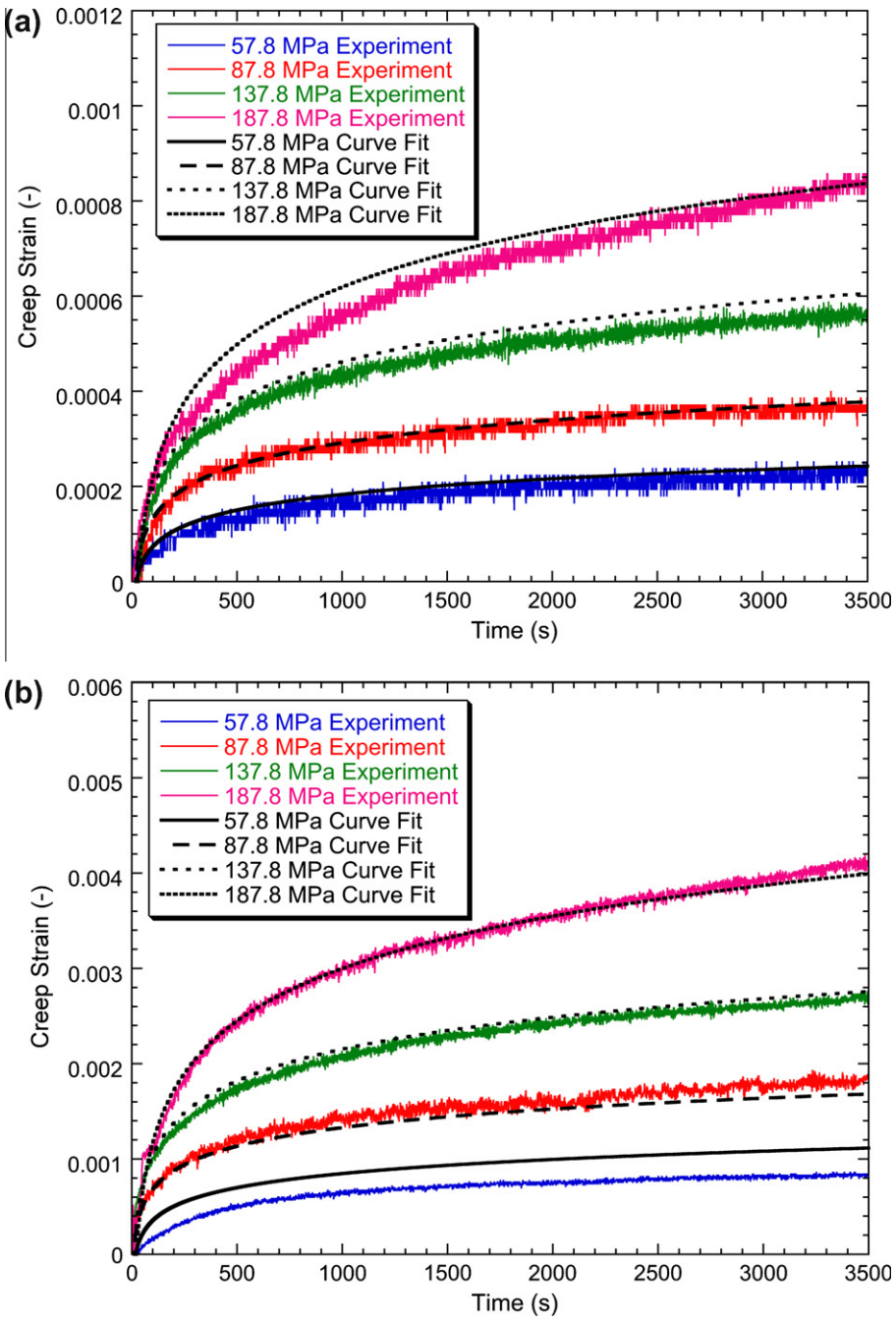

Fig. 4. Experimental creep strain data for the Cu foil, obtained at temperatures of (a) 25 °C and (b) 50 °C.

penetration depth, using an area function, which is dependent on the shape of the indenter. In practice, such a procedure may be unreliable, particularly if there is a substantial degree of pile-up. In the modelling work presented here, the area of contact, at a given applied load, was established as an output of the model, whereas the experimental value of the hardness was calculated automatically using software supplied by the manufacturer of the system (MML), in conjunction with the AFM-determined indenter shape function (for a sphere of radius 13 μm).

3.3. Experimental data and model predictions

3.3.1. Creep relaxation and the generation of residual stresses by quenching

Simulation of the creep relaxation at elevated temperature (Section 3.1) confirmed both that the stress state was always approximately uniform throughout (i.e. that edge effects occur only in small regions at the periphery of the specimen) and that full relaxation occurred well within the holding period of 1 h, even at the lowest holding temperature employed (50 °C). This is illustrated by the

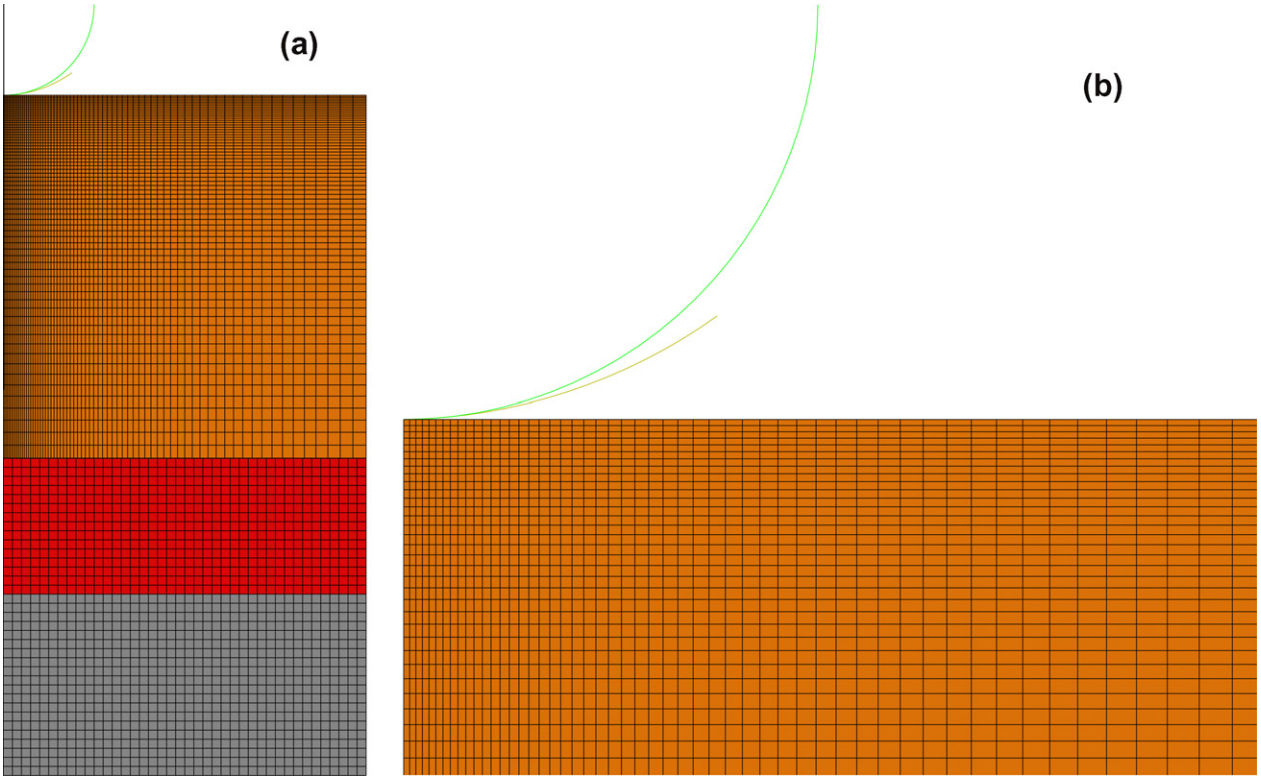

Fig. 5. Finite-element mesh for (a) the whole indentation model, including a 15 μm thick araldite layer (red) and the substrate (grey), and (b) a close-up of two indenter profiles—the green profile represents an ideal 10 μm radius sphere, while the yellow profile was obtained by AFM measurements on the actual tip. (For interpretation of the references to colour in this figure legend, the reader is referred to the web version of this article.)

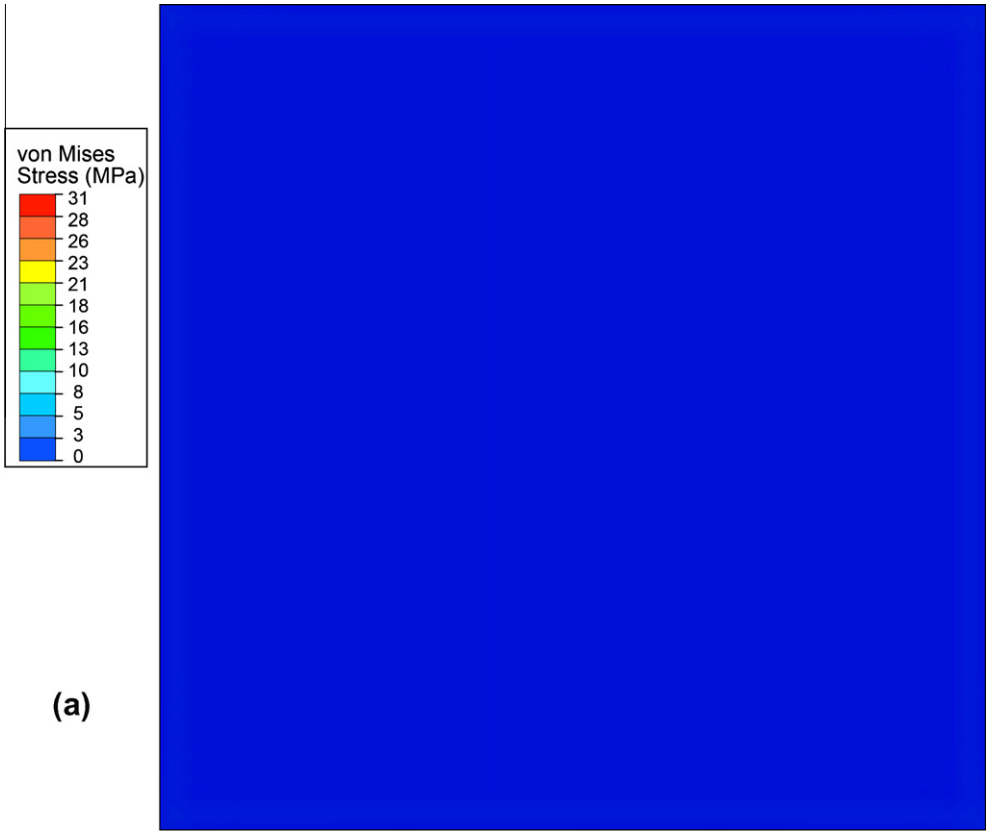

Fig. 6. Predicted von Mises stress as a function of position on the surface of the Cu foil after (a) heating from a stress-free state (at room temperature) to 50 °C and holding at that temperature for 60 min, and (b) quenching from a stress-free state at 225 °C to 25 °C and (c) holding for a further 10 min at 25 °C. (For an equal biaxial stress state, such as is created here, the von Mises stress is numerically equal to the two in-plane stresses.).

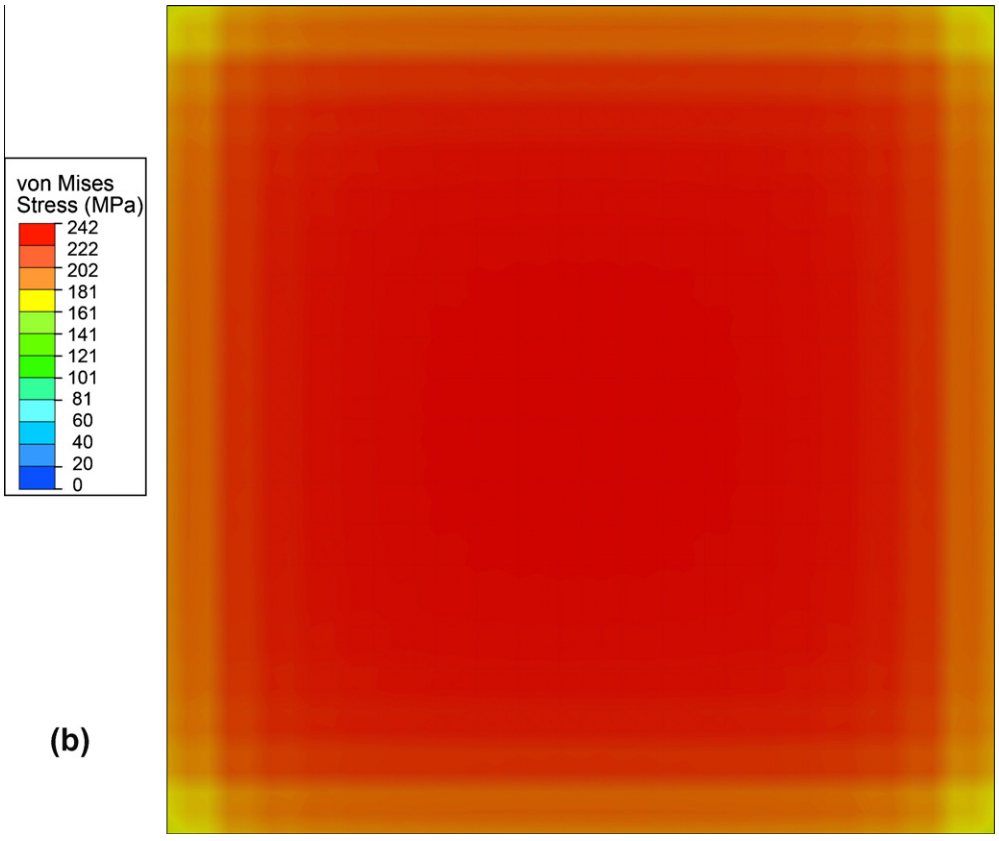

Fig 6. *(continued)*

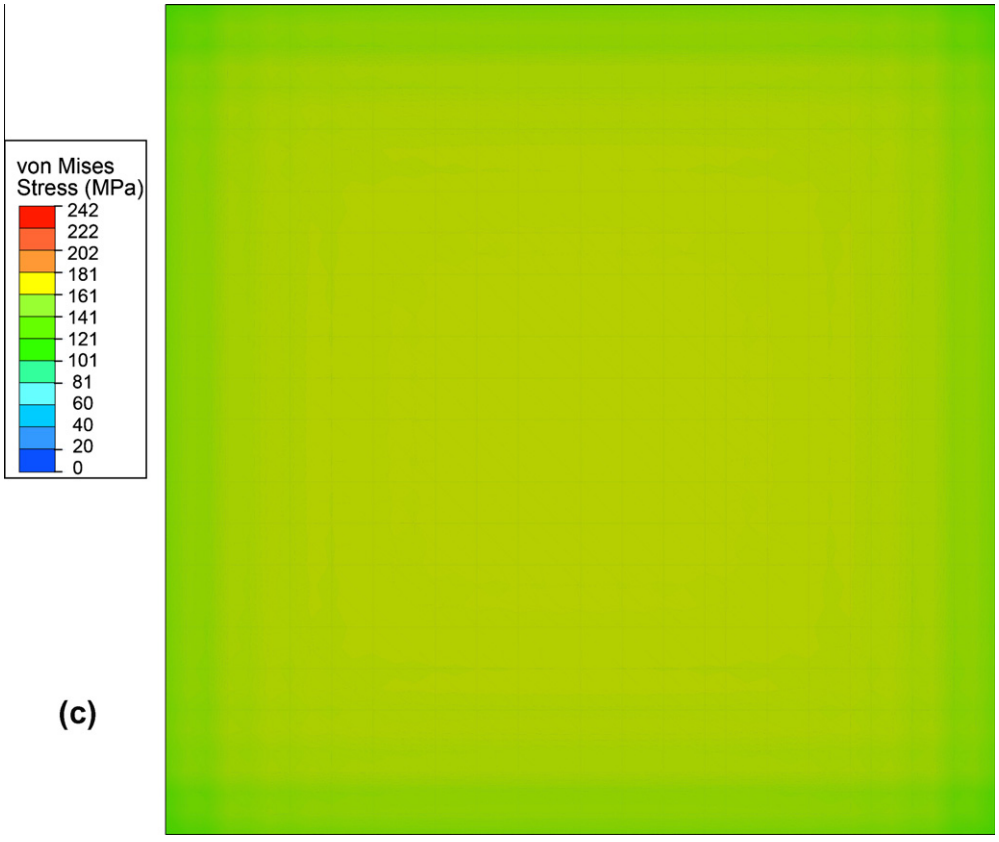

Fig 6. *(continued)*

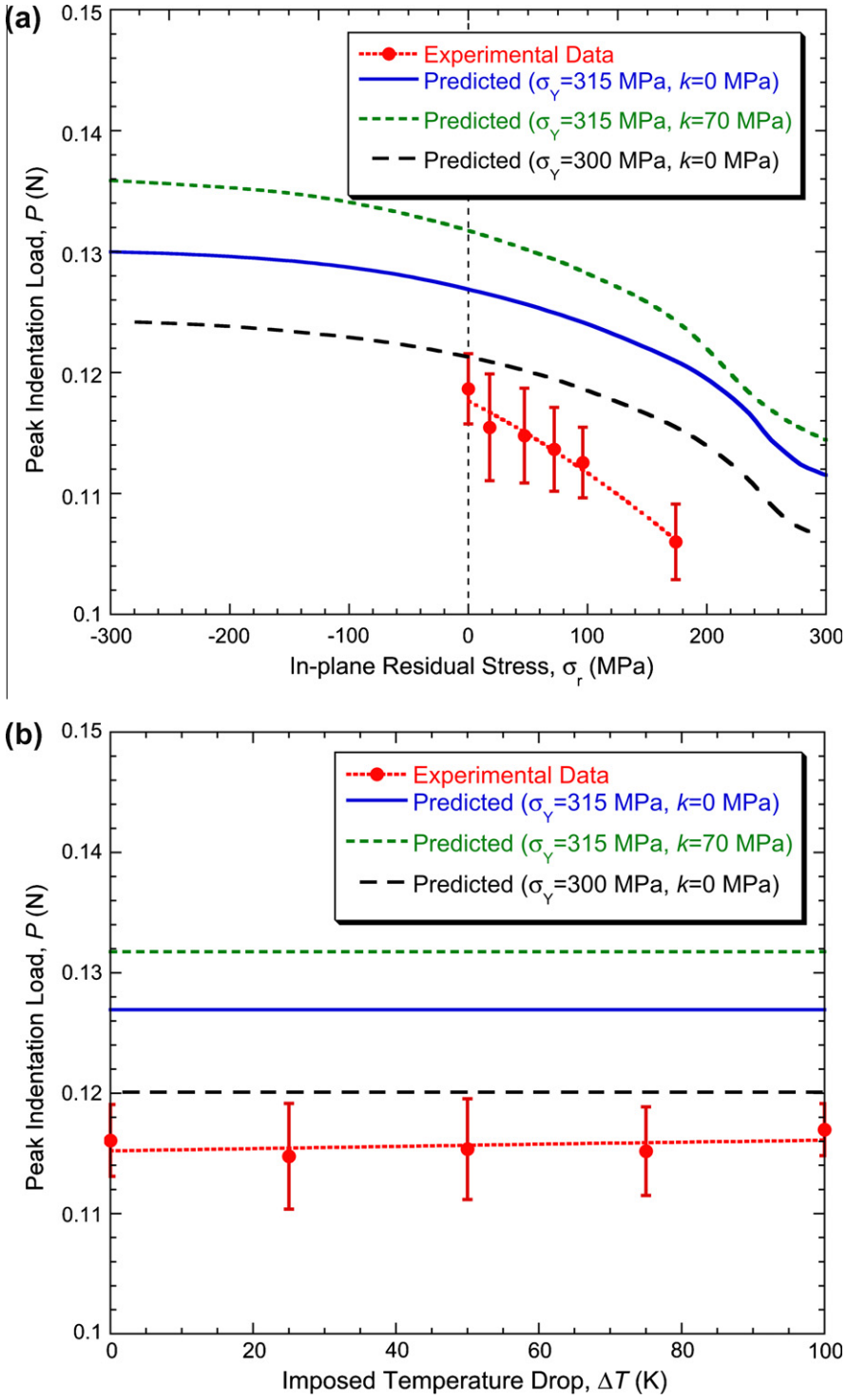

Fig. 7. Predicted and measured dependence of the peak indentation load (needed to generate a penetration depth of 1.65 μm at a loading rate of 10 mN s^{-1}), as a function of the in-plane (tensile) residual stress (generated by quenching from a temperature at which the system was stress-free), for (a) Cu foils on Ti substrates and (b) Cu foils on Cu substrates (for which no residual stresses were created).

predicted stress field shown in Fig. 6a, which relates to this case.

At room temperature, on the other hand, after quenching from elevated temperature, the relaxation that occurred within a period of 10 min was relatively limited. Fig. 6b shows the predicted stress field immediately after quenching by 200 K, while Fig. 6c shows how these stresses have been reduced by the relaxation that occurs during 10 min at room temperature. It can be seen that the initial stress level of about 250 MPa is reduced by this creep relaxation

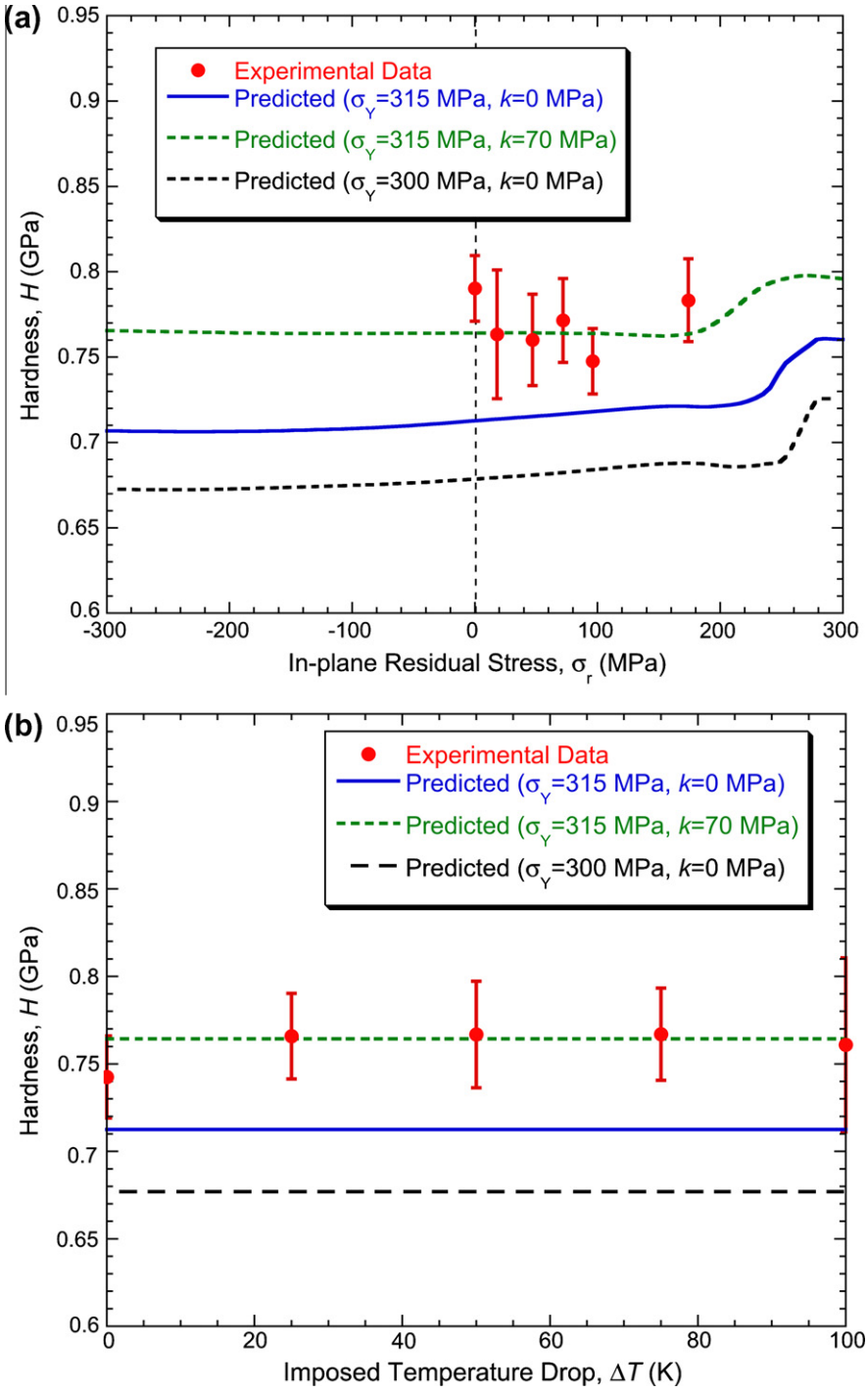

Fig. 8. Predicted and measured dependence of the hardness, as a function of the in-plane (tensile) residual stress (generated by quenching from a temperature at which the system was stress-free), for (a) Cu foils on Ti substrates and (b) Cu foils on Cu substrates (for which no residual stresses were created).

to about 174 MPa. In fact, after this initial period, the rate of relaxation falls off and the stress level would have been close to this throughout the indentation testing. Similar FEM runs were carried out for the other cases studied experimentally. The outcome of these runs, in terms of the predicted residual stress level present during the indentation testing, is shown in Table 1.

3.3.2. Peak indentation load

In Fig. 7, measured values of the peak indentation load (required to generate a penetration depth of 1.65 μm) are compared with predictions from the FEM model. Fig. 7a presents data for Cu foils on Ti substrates, as a function of the residual stress, while Fig. 7b shows corresponding data for Cu foils on Cu substrates (in which case there

are no residual stresses and, as expected, no consistent dependence of measured load on prior temperature change). The absolute values obtained for the Cu on Ti specimens are consistent with predictions from the model, as is the gradient, which reflects the sensitivity of the peak indentation load to the residual stress level. The data suggest that the actual yield stress in compression is a little lower than that estimated experimentally using the Cu foil disks.

Two sensitivity-related points should be noted about Fig. 7a in the context of using the present methodology to infer residual stress levels from measured indentation loads (to reach a specified depth). The first is that the absolute value of such an inferred residual stress level is very sensitive to both the yield stress and the work-hardening rate. For example, if the measured load had been, say, 120 mN, then the inferred residual stress would be $\sim$50 MPa for $\sigma_Y = 300$ MPa (and no work hardening), but would rise to $\sim$200 MPa for $\sigma_Y = 315$ MPa. Similar changes would arise from relatively small differences in work-hardening rate. This high sensitivity to material properties (which, incidentally, is a major advantage when measuring them via nanoindentation [10]) is likely to limit the accuracy to which absolute values of residual stress can be obtained in this way. Even with a well-characterized material (i.e. with the yield stress known to within about 1–2%), it seems likely that a precision level of better that about $\pm$50% would be difficult to achieve.

The second point, however, is a rather more positive one. For a given material (i.e. well-defined, if not necessarily well-known, values of σ_Y and k), the sensitivity of the measured load to the residual stress level (i.e. the gradient of the "correct" predicted line in Fig. 7a) is also relatively high, at least for tensile stresses. For example, a rise in (tensile) residual stress level from 0 to 200 MPa would induce a reduction in measured load of around 10 mN, i.e. approximately a 10% change, which should be detectable experimentally. This means that, while there might be a relatively high level of uncertainty about the absolute magnitudes of inferred residual stress levels, point-to-point variations should be detectable, making the technique suitable for mapping purposes. Of course, one of the main attractions of using a nanoindenter to monitor residual stresses lies in its excellent "lateral resolution", particularly when compared with alternative methods, so this is a significant point.

It is also worth noting that the predicted sensitivity of the required load to the residual stress level differs for compressive and tensile stresses, being greater when they are tensile. The sensitivity also increases as the (tensile) yield stress is approached. These effects can be understood in terms of the initial stress state (noting that the through-thickness stress is zero) and the way that the deviatoric component of the stress state changes as the through-thickness load is increased.

3.3.3. Indentation hardness

In Fig. 8, measured values of the hardness are compared with FEM predictions, for a range of imposed residual stress levels. For the foils on Ti substrates (Fig. 8a), it is both predicted and observed that the load necessary to reach the specified indentation depth shows little sensitivity to residual stress level, at least over most of the range. For residual stresses levels approaching the yield stress, some sensitivity arises, with the work-hardening rate also having an effect. This is related to pile-up formation, and its effect on the measured hardness. In fact, by considering Fig. 7a together with Fig. 8a, it can be seen that, since Fig. 8a effectively plots the ratio of the final load (as shown in Fig. 7a) to the contact area, the latter must be progressively falling as the residual stresses become more tensile. This is due to increased pile-up. It can also be seen that this effect is sensitive to the presence or absence of work hardening. In any event, it is clear from the characteristics shown in Fig. 8a, including the level of scatter in the experimental data, that the use of hardness measurements to obtain information about residual stress level is unlikely to prove fruitful.

For the Cu–Cu specimens, the experimental data do not show any clear dependence on the prior thermal history, as predicted, and the level of scatter again appears to be somewhat higher than for the peak load measurements.

4. Conclusions

Copper foils have been attached to massive Cu and Ti substrates, using a thin layer of a high-strength, high-temperature adhesive. Equal biaxial residual stresses (tensile) were generated within the foils in a controlled manner, by first heating to a selected temperature, holding at that temperature until creep deformation had led to complete stress relaxation and then quenching back to room temperature, and carrying out the nanoindentation. It was confirmed via FE modelling that the hold periods employed at high temperature were sufficiently long to ensure complete stress relaxation. At room temperature, on the other hand, after quenching, there was limited (but not negligible) stress relaxation during the short period prior to testing. FEM was therefore used to estimate the residual stress level at the time when the indentation testing was carried out. The following conclusions can be drawn from the work.

(i) The peak indentation load (required to reach a specified depth) was found to be fairly sensitive to the presence of (tensile) residual stresses, and to be a reasonably robust and reproducible parameter. Provided a suitable FE model is available, the residual stress level can be inferred from such a measured load. While no attempt has been made in the current work to measure an unknown residual stress in this way, the results presented here do indicate that this should be a viable procedure.

(ii) More specifically, with a transversely isotropic (equal biaxial) residual stress state and a spherical indenter (such that a single value is being inferred), as in the methodology of the present study, the expected precision to which the absolute value of a residual stress could be obtained is probably of the order of $\pm 50\%$, for tensile stresses. Even this level of accuracy would require the yield stress and initial work-hardening rate to be known to within something like $\pm 2\%$. Furthermore, the sensitivity is predicted to be even lower if the residual stresses are compressive. It is also necessary to be aware that creep may influence the observed behaviour, although in many cases it should be possible to ensure that it does not introduce significant errors into the deduction of residual stress levels.

(iii) While the high sensitivity of the measured load to the yield stress and, to a lesser extent, the work-hardening rate, limits the accuracy to which absolute levels of residual stress can be inferred, these measurements should reflect point-to-point variations in residual stress level in a given material. The technique is thus well-suited to mapping of residual stresses over the surface of a component (provided the microstructure, and hence the yield stress, are uniform throughout). Of course, nanoindentation involves interrogation of relatively small volumes of material, which is clearly an advantage for mapping purposes.

(iv) The region being interrogated is typically a few tens of microns in lateral extent and a few microns in depth. The surface finish therefore needs to be relatively smooth in order for the procedure to be viable. Furthermore, any oxide film present must be thin on this scale (i.e. $\ll 1\ \mu m$). Also, the indent should straddle at least several grains. However, there is no real barrier to the scale of the operation being raised substantially, making the constraints on surface finish, grain size and oxide film thickness less demanding, provided the load measurement system is sufficiently accurate over the necessary load range.

(v) Attempting to use the hardness as a measured parameter led to difficulties, since the sensitivity is lower and less consistent, and there are also complications relating to the exact way that hardness is defined, and the influence of pile-up formation on the area of contact. These difficulties may explain why previous attempts to obtain information about residual stresses from hardness measurements have in general been unsuccessful. Nevertheless, experimental data obtained in the present study are consistent with modelling predictions, although it is still concluded that this is unlikely to be a reliable method of measuring residual stress levels.

Acknowledgements

Financial support has come from AWE. There have been useful collaborations and discussions with several researchers from this establishment, particularly Dr. Andrew Wallwork.

References

[1] Tsui TY, Oliver WC, Pharr GM. J Mater Res 1996;11:752–9.
[2] Sines G, Carlson R, ASTM Bull 180; 1952.
[3] Taljat B, Pharr GM. In: Vinci R, Kraft O, Moody NR, Shaffer E, editors. Thin films: stresses and mechanical properties VIII. Mater Res Soc; 2000. p. 519–24.
[4] Swadener JG, Taljat B, Pharr GM. J Mater Res 2001;16:2091.
[5] Bolshakov A, Oliver WC, Pharr GM. J Mater Res 1996;11:760–9.
[6] Xu Z-H, Li X. Acta Mater 2005;53:1913–9.
[7] Suresh S, Giannakopoulos AE. Acta Mater 1998;46:5755–67.
[8] Lepienski CM, Pharr GM, Park YJ, Watkins TR, Misra A, Zhang X. Thin Solid Films 2004;447–448:251–7.
[9] Lee Y-H, Kwon D. Scripta Mater 2003;49:459–65.
[10] Dean J, Wheeler JM, Clyne TW. Acta Mater 2010;58:3613–23.
[11] ABAQUS user manuals, version 6.9.; 2009.
[12] Yu XX, Crocombe AD, Richardson G. Int J Adhes Adhes 2001;21:197–210.